Designing Thread forming Rotary Atomizers by Similarity Trials

A. Mescher*, P. Walzel
Laboratory of Mechanical Process Engineering, Technical University of Dortmund, Germany
axel.mescher@bci.tu-dortmund.de and peter.walzel@bci.tu-dortmund.de

Abstract

Rotary atomizers operated in the regime of laminar thread disintegration can be used for the production of sprays with narrow distributed droplet sizes. The liquid threads formed are attenuated due to centrifugal acceleration and small drop sizes can be achieved, compared to the thread detachment diameter. LAMROT atomizers can hold the desired break-up mode for an extensive range of liquid feed rates and revolution rates. This kind of rotary atomizer has a low plugging tendency and can be designed according to the principles described in [1]. For process design the mean drop size $d_{50,3}$ of the spray and the droplet *span*, representing the width of the droplet size distribution (DSD), have to be known. Empirical correlations are frequently used for the calculation of these parameters. However, such kind of correlations are often restricted to a specific atomizer geometry, to specific operating conditions respectively. Therefore similarity trials were carried out, covering a wide range of typical operating conditions for liquid thread break-up at rotary atomizers. The main influences on the thread break-up, like e.g. the gas-liquid interaction during thread break-up, were identified and separately varied. It is shown that the results of the similarity experiments can be used for elaborating empirical correlations for mean drop size and *span*, that are also valid for thread break-up at rotary atomizers.

These correlations can be applied to the design of spray processes including spiraling thread disintegration. As an example the design of a spray drying process including a LAMROT atomizer will be discussed.

Introduction

The industrial production of granules and powders from liquid feed is often performed via spray drying. Especially the atomizer-type has a significant influence on the process and is responsible for many quality-parameters of the process. On the one hand the formulated product needs to fulfill the required specifications in size distribution and structure, and on the other hand the drying process has to be easy operable. E.g. liquid feeds with a tendency to plugging have to be atomized reliably, in order to achieve the required product quality and process efficiency also for long running periods. Laminar operated rotary atomization is a proper method to gain both, high product quality, especially narrow droplet- and particle size distributions (PSD), and feasible atomization of problematic liquid feeds with plugging tendency.

In LAMROT atomization the liquid feed is distributed into multiple laminar open-channel-flows [1], see **Figure 1**. After detachment, the liquid forms thin threads, subsequently extended and attenuated by centrifugal acceleration. Thread break-up is caused by capillary instability (Rayleigh-breakup), leading to narrow distributed droplets. The breakup of attenuated threads leads to small droplet diameters ($d_{50,3}$) compared to the detachment diameter of the thread. Thus small particle diameters can be achieved even by atomizers with large bores. High throughput atomizers with multiple stages of bores have also been approved [2].

The geometry of this atomizer type can be designed according to the principles described in [1]. However, for process design the mean drop size as well as the width of the size distribution have to be known. Physical models as well as empirical correlations can be used for calculation of the drop sizes. Both options exhibit specific advantages and disadvantages.

Gramlich formulated a physical model for the break-up of spiraling threads. His model includes the influence of the liquid properties, the attenuation of the threads as well as the liquid/gas interaction, and allows for the calculation of the mean drop size from spiraling threads [3]. However, the break-up length of the spiraling thread is one parameter of Gramlich's model and has to be elaborated from experiments. Wallwork et al. described the break-up of inviscid spiraling threads via linear stability analysis [4]. The case of viscous spiraling threads is discussed in [5]. Models, based on linear stability analysis, allow for the calculation of mean drop sizes and give no information about the polydispersity of the droplet size distribution. The appearance of smaller satellite droplets from thread break-up can be incorporated by considering nonlinear effects. Părău et al. described the nonlinear stability of inviscid [6] and viscous spiraling threads [7]. Even though the size of satellite and main drops can be calculated from the models mentioned, no droplet size distribution can be gained and the solving effort is comparatively high.

Alternatively empirical correlations can be used for the calculation of the drop size. On the one hand empirical models are limited to a range of operating conditions validated by experiments. On the other hand correlations allow for an easy calculation of the desired drop sizes. In addition the width of the size distribution and

* Corresponding author: axel.mescher@bci.tu-dortmund.de

break-up lengths can also be correlated. It can be stated that empirical correlations are an alternative to physical modeling, if the experimental effort is acceptable.

In [8] we discussed the similarity of spiraling thread disintegration to the break-up of threads stretched in the field of gravity. The similarity to spiraling threads can be achieved in the field of gravity at distinctly lower acceleration/velocity of the threads and at a larger length scale. Due to the large scale and low velocity of the similarity experiments, the characterization of the thread break-up and the measurement of the PSD requires only moderate effort. **Figure 1** shows a rotary atomizer in section view, as well as shadowgraphic images of spiraling thread disintegration and of thread break-up in the field of gravity. The LAMROT atomizer (atomizer radius *R*: 50 mm) was designed according to [1]. The shadowgraphic image of spiraling thread break-up illustrates the gas-relative-velocity of the liquid threads. Assuming a low influence of air drag at the atomizer surface the gas-relative-velocity v_{rel} is given by the atomizer circumferential speed $R\omega$ [8]. The similarity experiments under gravity conditions also establish a gas-relative velocity between the stretched threads and the environmental air. For that reason the tubular nozzles were placed in a transparent wind tunnel.

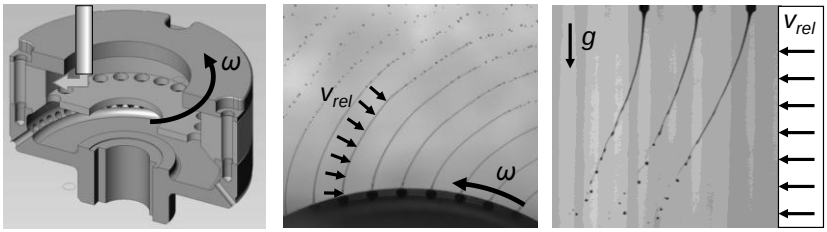

Figure 1: left: Section view of a rotary atomizer with 60 bores and radius 50 mm. Center: disintegration of spiraling threads. Right: Disintegration of threads stretched by gravity

The break-up of stretched liquid threads in the field of gravity was extensively investigated for numerous flow conditions and liquid properties, see also [9]. Due to the similarity of the systems, these correlations can also be used for spiraling thread break-up. In the present work the similarity experiments in the field of gravity are described and empirical correlations for mean drop size and width of the size distribution (*span*) are introduced and compared to the break-up of spiraling threads.

Experiments and Methods

The breakup of stretched threads emerging from rotary atomizers or from tubular nozzles in the field of gravity can be described by nondimensional numbers. The nondimensional droplet size $d^* = d_{50,3} / L_C$ is defined as the ratio of the break-up length to the capillary length L_C. The capillary length $L_C=\left(\sigma/\rho_l\, g\right)^{0.5}$ was found to be a suitable characteristic length scaling the breakup process from stretched liquid threads [10, 11], as it relates capillary forces to the field forces responsible for the thread acceleration. The drop size from stretched liquid threads was found to be practically independent of the nozzle diameter *D*, as the thread diameter after detachment primarily depends on the thread attenuating acceleration. Schneider found negligible deviations of the drop size from stretched threads with detachment diameters from 2 mm < *D* < 16 mm [12]. The width of the droplet size distribution can be expressed in terms of the droplet *span*, defined as:

$$span = \frac{d_{90,3} - d_{10,3}}{d_{50,3}} \tag{1}$$

In [8] we demonstrated that thread break-up in the field of gravity is influenced by the nondimensional volumetric flowrate $\dot{V}^*$, the nondimensional viscosity μ^* and the gas-Weber-number We_g. $\dot{V}^*$ describes the influence of the flow momentum due to discharge and acceleration by gravity related to the capillary effect.

$$\dot{V}^* = \frac{\pi}{4} \cdot We^{0,5} Bo^{0,75} = \dot{V} \left(\frac{a^3 {\rho_l}^5}{\sigma_{lg}^5} \right)^{0,25} \tag{2}$$

The viscosity parameter μ^* represents the influence of viscous shear within the two-phase system.

$$\mu^* = \mu \left(\frac{a}{\rho_l \sigma_{lg}^3} \right)^{0.25} \tag{3}$$

Due to the use of the capillary length L_C as characteristic length, the nondimensional viscosity number μ^*, is adequate to an Ohnesorge number *Oh* and can also be defined as:

$$\mu^* = Oh_{L_C} = \frac{\mu_l}{\sqrt{\sigma_{lg} \rho_l L_C}} \tag{4}$$

The influence of the environmental air and its interaction with the threads is characterized by a gas-Weber-number We_g, defined as the ratio of dynamic gas pressure, caused by the gas-relative-velocity (v_{rel}), and the capillary pressure. The characteristic length for the gas-liquid interaction is given by L_c.

$$We_g = \frac{v_{rel}^2 L_c \rho_g}{\sigma_{lg}} \tag{5}$$

Experiments on rotary atomization are carried out in a tubular test rig, see **Figure 2**. Backlight images of the thread break-up can be acquired and a sector shaped part of the spray cut out of the spray for droplet sizing via

laser-diffraction measurements (Malvern Spraytec, 300 mm lens). The laser-diffraction system was aligned secantially to the atomization plane in order to achieve a sufficient light obscuration for reliable measurements. A 150 mm secant of the spray was rayed by the laser and the light transmission varied between 7.5 and 15 %. The liquid properties can be adjusted with differently concentrated glycerol/water-mixtures. The liquid properties were measured according to the liquids used in the similarity trials, see next paragraph. The atomizer operation point can be controlled by adjusting the atomizer revolution rate and liquid feed flowrate.

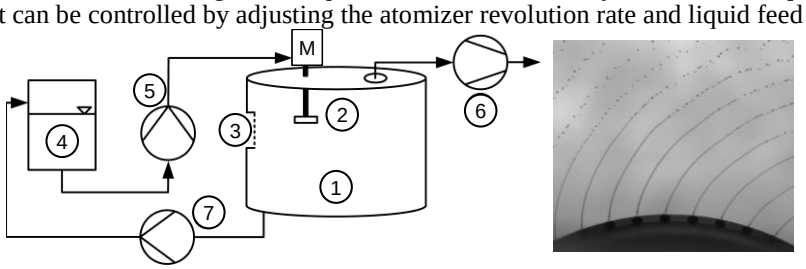

Figure 2: Test rig for the characterization of spiraling thread break-up at rotary atomizers. (1) steel vessel (2) atomizer (3) slit. The spray leaves the test rig here and can be investigated via laser-diffraction measurements (4) liquid hold-up (5) pump (6) exhaust (7) reflux pump. On the right a typical backlight image is shown.

The experimental setup for the similarity experiments in the field of gravity consists of a transparent channel and a backlight imaging equipment, see **Figure 3**. The setup allows observation and documentation of the breakup of stretched liquid threads under the influence of a gas cross-flow. An axial fan is provided to convey the environmental air through the channel and thus to induce the gas-relative-velocity on the threads. Up to three tubular nozzles with inner diameters of 6 mm < D < 14 mm can be mounted vertically in the ceiling of the channel. In the present work a nozzle diameter of 10 mm was used exclusively, because only minor influences of the nozzle diameter on the drop size and span were observed, see also [12]. The liquid is fed by a screw pump. Minor flow pulsations are eliminated by pressurized gas-buffers before the liquid detaches from the nozzle orifices. Water/glycerol mixtures were used in order to investigate the behavior of viscous threads. Glycerol mass fractions up to 93 % were employed ($\mu \approx 400$ mPas, $\sigma \approx 65$ mN/m, $\rho_l \approx 1250$ kg/m³). The liquid temperature was controlled and the liquid was dyed by black ink, with a volumetric content < 0.5 %, as a contrast agent to improve the identification of the contours of threads and drops. The liquid properties were recurrently measured. Surface tension measurements were carried out by a ring method, kinematic viscosity was metered by an Ubbelohde viscosimeter and the density was monitored by resonant frequency measurements. During the experiments, the flow-rate was continuously measured by a magnetic flow-meter and a rotameter (variable area flowmeter) and adjusted to flow-rates of up to 21 l/h per nozzle.

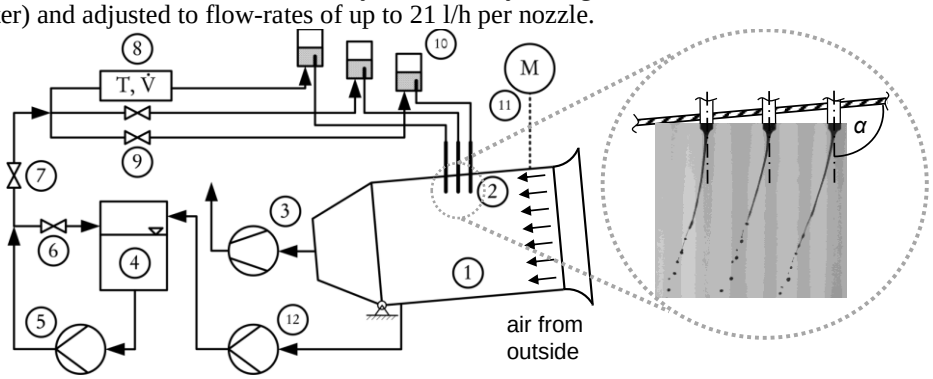

Figure 3: Sketch of the experimental setup. (1) Transparent PMMA channel, length: 1500 mm, height: 1000 mm, width: 120 mm. (2) Nozzles, up to three tubular nozzles (inner diameter: 6 mm < D < 14 mm) can be mounted vertically. (3) Environmental air can be conveyed through the channel. A constant gas relative velocity perpendicular to the thread axes is obtained. (4) Liquid tank: The temperature of the liquid is controlled. (5, 6, 7) The liquid flow is adjusted by a pump, a bypass and a pressure valve. (8) Measurement site of the liquid flow-rate and temperature. (9) Valves for flow-rate adjustment. (10) Buffers with gas hold-up providing flow without detectable pulse. (11) Motorized winch to adjust the angle between the gas flow and the vertical falling threads within 90° < α <110. (12) Reflux pump

The backlight images were processed by a Matlab-routine in order to extract the desired thread contour parameters like break-up length, break-up diameter, mean drop size and width of the DSD. In order to enhance the statistical accuracy, per experiment 100 pictures were acquired, corresponding to 300 threads and typically more than 5000 droplets. **Figure 3** also shows a typical backlight image. Even though a length-fluctuation of the single threads could be observed, the mean break-up lengths of the threads from the three nozzles were equal. The relative standard deviation of the break-up length was comparably small, typically below 5 % and always below 10 %. The gas cross-flow direction can be inclined to the vertically falling threads by tilting the whole channel. Angles of 90° < α <110° between the threads and the gas-flow direction can be obtained. The range of inclina-

tion angles investigated here was chosen with respect to typical spray drying conditions of laminar threads [1]. Even though the detachment direction is mainly tangentially oriented towards the rotary atomizer wheel in spray drying, a radial velocity component exists and the gas-flow-direction towards the spiraling liquid threads is slightly inclined, compare **Figure 1**.

Break-up of liquid threads stretched by gravity under gas-crossflow

In the present work the results are shown as a function of the gas-weber-number in order to illustrate the impact of the gas-crossflow on the stretched threads. The gas-liquid interaction was found to influence the break-up process at least as significant as e.g. liquid properties and liquid throughput.

Mean drop size

As an example, in **Figure 4** the nondimensional mean drop sizes are shown for two viscosities (μ = 35 mPas and μ = 300 mPas) and for different gas-Weber numbers. Experiments at different nondimensional volumetric flow-rates are presented. Increased nondimensional volumetric liquid flowrates were found to lead to larger droplets. The tendency to larger droplets at higher liquid flowrates can be explained by less attenuated threads with larger break-up diameters, due to the higher nozzle exit velocity. A tendency to larger drop sizes d^* for higher gas-relative-velocities was also found. **Figure 4** shows the nondimensional droplet size as a function of the gas-Weber number for different viscosities. **Figure 4** exemplifies the impact of the liquid viscosity on the mean drop size course at intensified gas-relative-velocities. For the case of low viscous liquids, as shown in **Figure 4** a), the drops distinctly increase in size in the range of $We_g < 0.5$, due to also significantly decreased break-up lengths. The increase of the drop size can be explained by larger break-up diameters of the threads due to shorter break-up lengths at higher We_g, data not shown. For significantly higher viscosities the course of the drop size at increased gas-Weber-numbers was found to be more complex, than shown in **Figure 4** a).

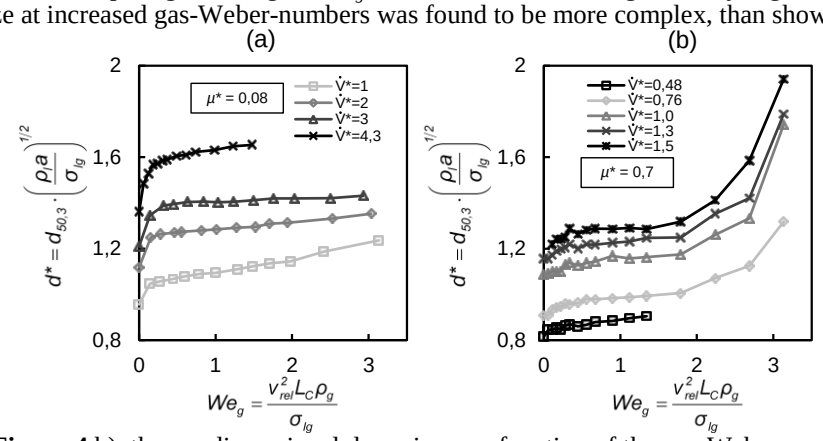

Figure 4: Nondimensional mean drop size from stretched threads for different gas-Weber numbers and nondimensional flowrates. Experimental parameters: nozzle inner diameters: D = 10 mm. Glycerol/water mixture, a) μ = 35 mPas, b) μ = 300 mPas.

In **Figure 4** b), the nondimensional drop size as a function of the gas-Weber-number is presented for comparably high viscous liquid (300 mPas). The drop size increases slightly in the range of low We_g, but strongly in the range of $We_g > 2$. The observed behavior in the range of $We_g < 2$ is comparable to the drop size course of lower viscous liquids, as the drop size increases more first and less afterwards. In contrast to lower viscosities, the observed strong increase of the drop size at $We_g > 2$ is not just caused by decreased break-up lengths. An altered break-up mode of the threads can be observed. The viscous and strongly attenuated threads are subject to a mainly non-axis-symmetric break-up in the range of high We_g. Large main droplets and thin ligaments in between are formed. **Figure 5** a) and b) show the break-up of spiraling threads at different operating conditions. In c) and d) the break-up of stretched liquid threads in the field of gravity and under gas-crossflow is shown. Especially for long spiraling threads a non-axisymmetric break-up occurs, see a). This break-up pattern was also found during the similarity trials in the field of gravity, see c) and d).

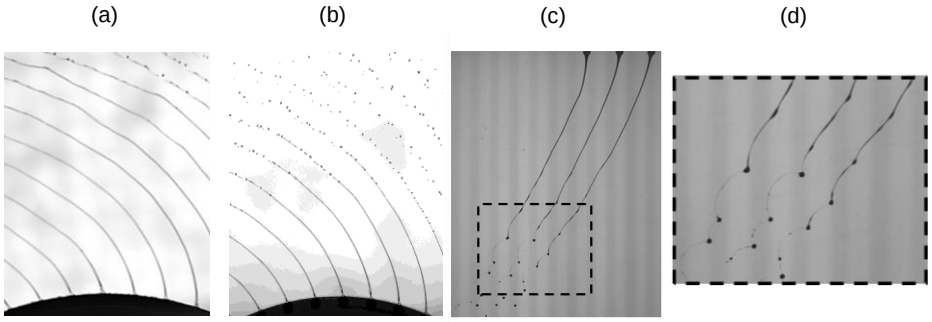

Figure 5: Break-up of laminar threads. (a) non-axisymmetric break-up mode (b) intended axisymmetric break-up mode. (c) Image of the thread break-up under gravity conditions and magnified break-up range (d). Except for (b) the drop formation is caused by mainly non-axis-symmetric disturbances.

The break-up pattern was found to depend on We_g, μ^* and $\dot{V}^*$. Low flowrates and high viscosities lead to long and thin threads, tending to non-axis-symmetric break-up even at lower We_g. Eq. 6 describes the critical gas-Weber-number $We_{g,crit.}$ characterizing the transition between the break-up modes. In **Figure 6** the experimentally observed break-up pattern, as well as the correlation for $We_{g,crit}$ are presented.

$$We_{g,crit.} = 1{,}92 \cdot \dot{V}^{*0{,}15} \cdot \mu^{*-0{,}39} \tag{6}$$

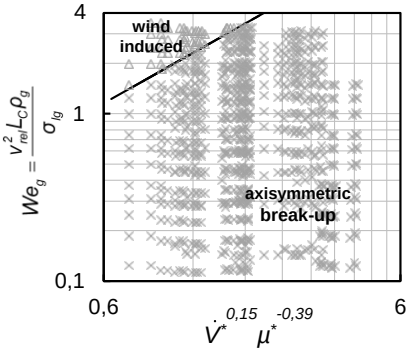

Figure 6: Critical gas-Weber-number. The solid line according to eq. 6 separates the observed break-up patterns into axis-symmetric break-up (crosses) and non-axis-symmetric break-up (triangles), see Figure 5 (c) and (d). Non-axis-symmetric break-up can be found at high We_g, especially for high viscosities and low flow-rates, with long, thin threads. Experimental parameters: 782 measurements. Glycerol/water mixtures, viscosity: 4.5 mPas < μ < 400 mPas, 0.01 < μ^* < 1.3, flowrate per nozzle: 1.4 l/h < $\dot{V}$ < 21 l/h, i.e. 0.48 < $\dot{V}^*$ < 6.4 and gas-Weber numbers: 0 < We_g < 4.8

The experimental data were also correlated in nondimensional form. The gas-relative-velocity v_{rel} is defined as:

$$v_{rel} = \left(v_l - \left(v_g \cdot sin(\alpha - 90°)\right)^2 + \left(v_g \cdot cos(\alpha - 90°)\right)^2\right)^{0.5} \tag{7}$$

v_l is the nozzle exit velocity of the thread and v_g is the velocity of the gas cross-flow affecting the thread with the inclination angle α, see **Figure 3**. For the correlation of the nondimensional mean drop size (eq. 8), the different break-up patterns were considered. The resulting equation is separated into a first part, describing the increase of the drop size in the axis-symmetric break-up regime, due to reduced break-up lengths (eq.9). See $We_g \lesssim 1.8$ in **Figure 4** b).

$$d^* = \begin{cases} d^*_{axisymm.}: We_g \le We_{g,crit.} \\ d^*_{wind-ind.}: We_g > We_{g,crit.} \end{cases} \tag{8}$$

$$d^*_{axisymm.} = 1{,}043 \dot{V}^{*0{,}259} \mu^{*0{,}038} \cdot \left(1 + 139{,}65 We_g\right)^{0{,}248\left(1+4{,}1\cdot 10^5 \mu^*\right)^{-0{,}206}} \tag{9}$$

The second part of the equation describes the increasing drop size in the non-axisymmetric break-up regime. When the critical gas-Weber-number according to eq. 6, is overcome the second term is added and the nondimensional mean drop size is calculated under consideration of the non-axis-symmetric effects, see $We_g \gtrsim 1.8$ in **Figure 4** b).

$$d^*_{wind-ind.} = d^*_{axisymm.}\left(We_{g,crit.}\right) + 1{,}151 \dot{V}^{*-0{,}071} \mu^{*0{,}942} \cdot \left(We_g - We_{g,crit.}\right)^{0{,}881} \tag{10}$$

For the calculation below $We_{g,crit.}$, a sum term for the influence of We_g was implemented to describe the case without gas cross-flow. In order to consider the different drop size courses for different viscosities, the exponent of We_g also depends on μ^*, compare **Figure 4** a) and b). **Figure 7** shows a comparison between experiments showing axis-symmetric break-up and calculated values for the nondimensional mean drop size d^* by eq. 9. In the axis-symmetric break-up regime the mean deviation between the experiments and the correlation is 2.02 %, while the maximum deviation is 9.9 %. 754 experiments showed an axis-symmetric break-up. The 28 results in the non-axis-symmetric break-up regime are not shown in **Figure 7**.

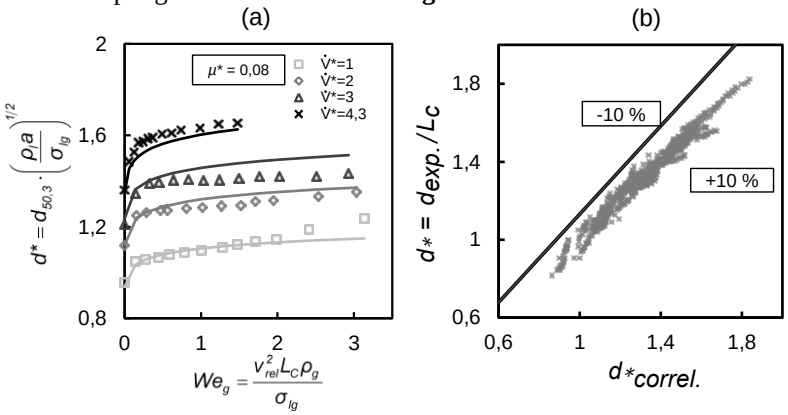

Figure 7: (a) Nondimensional mean drop size from stretched threads for different gas-Weber numbers. The solid lines represent the correlation according to eq. 9. Experimental parameters: nozzle inner diameters: D = 10 mm. Glycerol/water mixture, μ = 35 mPas. (b): Correlation of the nondimensional mean drop size. The solid lines represent the deviation from the ideal fit. 782 measurements, each consisting of 100 images with 3

threads per image, are plotted against the correlated values. The solid lines represent the deviation from the ideal fit. Experimental parameters: Three nozzles of an inner diameter of D = 10 mm were mounted. Glycerol/water mixtures, viscosity: 4.5 mPas < μ < 400 mPas, 0.01 < μ^* < 1.3, flowrate per nozzle: 1.4 l/h < $\dot{V}$ < 21 l/h, i.e. 0.48 < $\dot{V}^*$ < 6.4, gas-Weber numbers: 0 < We_g < 4.8

The values of all constants were globally fitted by a clustered non-linear GRG (generalized reduced gradient) optimization of the sum of residual-squares (MS Excel Solver). It has to be mentioned, that the deviation between experimental and correlated data is larger in that break-up regime. Under consideration of these results, the mean deviation of the correlation is 8.48 % and the maximum deviation is 37.8 %.

span of the DSD

Especially for technical applications based on the break-up of stretched threads, the width of the drop size distribution (DSD) is a very important quality aspect of the atomization process. Narrowly distributed droplets are easier to handle in processes, like e.g. spray drying. A low *span* of the DSD (eq. 1) is crucial for the production of a homogeneous product of high quality [13].

In **Figure 8** typical droplet *spans* for a low and a higher viscous liquid are shown for different gas-Weber numbers. Generally, the *span* was found to be insignificantly sensitive to the inclination angle of the gas cross-flow and to the liquid flow-rate.

The influence of viscosity was complex when a gas cross-flow is present. **Figure 8** a) shows the droplet *span* of a comparably low viscous liquid, while the more viscous case is shown in **Figure 8** b). For the case without gas cross-flow, viscosity affects the *span* moderately. However, a more uniform break-up mode and a slightly lower *span* value is observed for higher viscous liquids, when We_g is low. When increasing We_g, the droplet *span* of the higher viscous liquid increases to a larger degree compared to the lower viscous liquid. At high We_g, the thread break-up alters to a non-axis-symmetric mode, as shown in **Figure 5** and *span* values, even higher than observed for a less viscous liquid, can be found. The transition to the non-axisymmetric break-up mode according to eq. 6 was plotted as dashed line in **Figure 8** b).

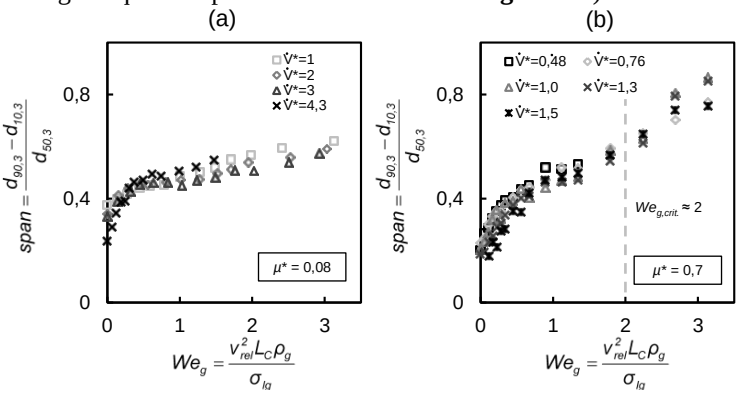

Figure 8: *span* of the DSD for different gas-Weber numbers and nondimensional flowrates. Experimental parameters: nozzle inner diameters: D = 10 mm. Glycerol/water mixture, a) μ = 35 mPas, b) μ = 300 mPas.

The experimental data was correlated in nondimensional form. Eq. 11 describes the best fit to the experiments. The *span* is given as a function of μ^* and We_g.

$$span = \left[1{,}61 - \exp\left(-5{,}44We_g - 0{,}605\right)\right] \cdot \left[0{,}099\mu^{*0{,}364}We_g + 0{,}183\mu^{*-0{,}128}\right] \quad (11)$$

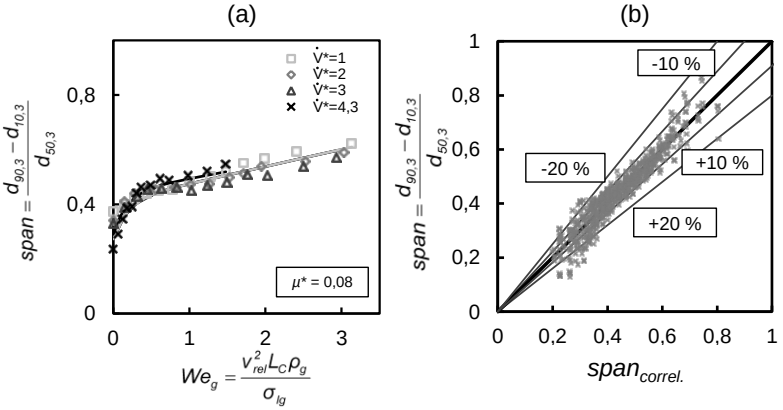

Figure 9: (a) *span* of DSD from stretched threads for different gas-Weber numbers. The solid lines represent the correlation according to eq. 11. Experimental parameters: nozzle inner diameters: D = 10 mm. Glycerol/water mixture, μ = 35 mPas. (b): Correlation of the nondimensional mean drop size. The solid lines represent the deviation from the ideal fit. For experimental parameters see **Figure 7**.

In **Figure 9** a comparison between experiments and calculated *span* values from eq. 11 is shown. The mean deviation between the experiments and the correlation is 8.48 %, while the maximum deviation is 106.5 %. As it can be seen from **Figure 9** a), the *span* value can be predicted quite well. The course of the *span* value is predicted accurately for low viscosities as well as for higher viscous liquids. However, especially at conditions leading to a narrow DSD and low *span* values the correlation lacks accuracy, e.g. at low gas-relative-velocities. In the range of higher gas-relative-velocities, as occurring in typical technical applications of stretched threads the accuracy of eq. 11 is better.

Comparison of thread break-up under gravity conditions to spiralling thread break-up

During the experiments on gravity stretched threads the influence of the liquid flow-rate, the liquid properties and the gas cross-flow were chosen close to the spiraling thread break-up at laminar operated rotary atomizers. The experimental results obtained in the similarity trials will be discussed with respect to this kind of rotary atomization, where the acceleration of gravity is replaced by the centrifugal acceleration. The empirical correlations obtained from the similarity experiments will be compared to drop size data from experiments on rotary atomization, in order to check their validity for spiraling thread break-up.

In numerical studies of spiraling threads Decent et al. [5] found decreased droplet sizes, when increasing viscosity. For low revolution rates of the threads, a monotonic decrease of the drop size with increasing viscosity is predicted. This dependency was explained by an increased break-up length of the stretched threads leading to smaller break-up diameters. At higher revolution rates of the threads, Decent et al. calculated a non-monotonic behavior with increasing viscosity. The drop size first increases, due to the damping effect of viscosity towards small wavelength disturbances. At further increased viscosities the drops are predicted to become smaller, again due to longer and thus more attenuated threads. In addition to the prediction by Decent et al., concerning the impact of liquid viscosity on the break-up of spiraling threads, our experiments in the field of gravity indicate a combined influence of a gas cross-flow and liquid viscosity. As shown in **Figure 4** the influence of a perpendicular gas-relative-velocity was found to be comparably complex and to lead to unexpected behavior of the drop size course in the field of gravity.

For threads stretched by gravity, increased values of We_g were found to lead to larger *span* values. At high values of We_g a fully altered break-up mode was observed and the *span* increases distinctly, see **Figure 5** and **Figure 8**. Gramlich and Wong et al. also reported on a ligament formation preceding the droplet formation, for the case of intensified aerodynamic interaction between viscous spiraling threads and the environmental gas [3, 14]. The spray generated by LAMROT atomizers also results in increased values of the droplet *span* for a higher rotation rate, i.e. an operating condition with a higher gas-relative-velocity of the spiraling threads, see also [15]. With respect to the results of the present study, aerodynamic effects can therefore clearly be identified to promote the appearance of a non-axis-symmetric break-up mode and to raise the *span* for the case of spiraling threads. In **Figure 10** experimental results from rotary atomization ($a = R\omega^2$) are shown and compared to the correlations formulated from the similarity experiments in the field of gravity ($a = g$). The nondimensional mean drop size is shown as a function of the gas-Weber number. We_g is defined with the atomizer circumferential velocity $u = R\omega$ in order to describe the gas-relative-velocity of the spiraling threads. The nondimensional mean drop size as well as the *span* increase at higher We_g. This was also found in the similarity experiments under gravity conditions. **Figure 10** shows the coincidence of the similarity experiments and spiraling thread break-up and the validity of the correlations for the chosen atomization parameters, even though the value of the nondimensional flowrate $\dot{V}^*$ is outside the range investigated in the similarity experiments.

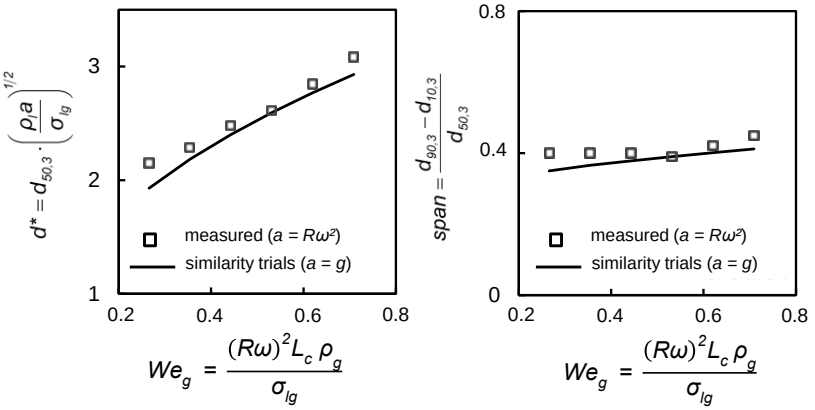

Figure 10: nondimensional drop size d^* and droplet *span* for different gas-Weber-numbers We_g. Comparison of rotary atomization experiments to calculated values. Experimental condition: Glycerol/water-mixture, viscosity μ = 24 mPas, atomizer diameter D = 66,6 mm, 40 threads per atomizer, liquid flowrate: 14,2 l/h, atomizer speed: 3000 < n < 8000 rpm, Nondimensional operating conditions: 0,24 < μ^* < 0,4 and 9,4 <$\dot{V}^*$< 42.

However, for distinctly higher viscous liquids or for distinctly higher liquid flowrates the match of correlation and experiment was found to be less satisfying. Fur such operating conditions the break-up length of the spiraling threads increases strongly in size and coalescence occurs. In the range of nondimensional numbers, that was investigated during the similarity experiments (see **Figure 7**), the relative standard deviation between correlation and experiments was 24 % (d^*) and 32 % (*span*). The empirical correlations achieved from the similarity experiments may therefore be a helpful tool for the design of thread forming rotary atomizers.

Summary and Conclusions

Experiments on the break-up of stretched liquid threads, exposed to a gas cross-flow, were carried out as similarity trials for the characterization of spiraling thread break-up. The present work demonstrates the minor influences of the inclination angle of the gas cross-flow on the break-up lengths and DSD. Viscosity and liquid flowrate were confirmed to be important influence-parameters on the break-up process. Intensified gas cross-flows were found to lead to a decreasing break-up length. The mean drop size from stretched liquid threads was found to increase at higher gas-relative-velocities. In the range of low gas-relative-velocities an increasing diameter of the shorter threads could be identified to cause the larger drops. At high cross-flow intensities and especially for thin threads a fully altered non-axisymmetric break-up mode occurs. However, as the present study did mainly focus on the axisymmetric break-up, comparatively few experimental results on the non-axisymmetric break-up were gained. Correlations for the mean-drop size and the *span* of the DSD were formulated. On the one hand these correlations may facilitate a future comparison to numerical results. On the other hand especially the correlations for drop size and width of the DSD can be used to quantify the influence of the gas cross-flow in spiraling thread disintegration, e.g. rotary atomization in spray drying.

The spiraling threads in spray drying applications are typically subject to a gas-influence close to the conditions investigated in the present work. The gas-relative-velocity here consists of a component caused by the atomizer circumferential speed, as well as of a component caused by the axial heating gas supply through an annular slit above the atomizer. For example: rotary atomizer with 500 bores, diameter 100 mm running at 6000 rpm, liquid: ρ_l = 1180 kg/m³, μ = 20 mPas, σ = 69 mN/m, liquid flowrate $\dot{V}$ = 100 l/h, axial heating gas supply: ρ_g = 1 kg/m³, gas-relative-velocity of the threads velocity v_{rel} = 30 m/s, resulting in $\dot{V}^*$ =18,1, μ^* = 0.3 and We_g = 0.7. For such conditions it can be stated that mean drop size as well as the *span* can be estimated according to the presented correlations.

Acknowledgements

The authors want to thank the DFG (Deutsche Forschungsgemeinschaft) for the financial support of our research within the SPP 1423 “Prozess-Spray”.

References

[1] T. Schröder, P. Walzel, *Chem. Eng. Technol. 21-4*, 349-354, (1998).

[2] P. Walzel, G. Schaldach, H. Wiggers, *International Conference on Liquid Atomization and Spray Systems*, Como Lake, Italy, 8 - 10 September 2010.

[3] S. Gramlich, Numerische und experimentelle Untersuchungen zum Zerfall feststoffbeladener Flüssigkeitsstrahlen im Zentrifugalfeld, *Dissertation*, Universität Stuttgart, (2011).

[4] I. M. Wallwork, S. P. Decent, A. C. King, R. M. S. M. Schulkes, *J. Fluid Mech. 459-1*, 43-65, (2002).

[5] S. P. Decent et al., *App. Math. Mod. 33*, 4283–4302, (2009).

[6] E. I. Părău et al., *Wave Motion 43-7*, 599-618, (2006).

[7] E. Părău et al., *Journal of Engineering Mathematics 57-2*, 159-179, (2007).

[8] A. Mescher, P. Walzel, ILASS - Europe 2010, 23rd Annual Conference on Liquid Atomization and Spray Systems, Brno, Czech Republic, 5 - 8 September 2010.

[9] A. Mescher, A. Möller, P. Walzel, ILASS - Europe 2011, 24rd Annual Conference on Liquid Atomization and Spray Systems, Estoril (P), 05. – 07. September 2011.

[10] P. Bär, Über die physikalischen Grundlagen der Zerstäubungstrocknung, *Dissertation*, TU Karlsruhe, (1935).

[11] J. Eggers, T. F. Dupont, *J. Fluid Mech. 262*, 205 - 21, (1994).

[12] S. Schneider, P. Walzel, *ILASS-Europe*, Toulouse, 5th - 7th July.

[13] P. Walzel, *Chem. Eng. Technol. 34-7*, 1039-1048 (2011).

[14] D. C. Y. Wong et al., *Int J Multiphas Flow 30*, 499–520, (2004).

[15] A. Mescher, P. Walzel, *17th International Drying Synposium*, Magdeburg, Germany, 3-6 October 2010.